Experimental and Theoretical Study of the Reaction of F2 with Thiirane

Yuri Bedjanian, Antoine Roose, Valérie Vallet, Manolis Romanias

molecules

MDPI

Article

Experimental and Theoretical Study of the Reaction of F_2 with Thiirane

Yuri Bedjanian [1,*], Antoine Roose [2], Valérie Vallet [3] and Manolis N. Romanias [2]

[1] Institut de Combustion, Aérothermique, Réactivité et Environnement (ICARE), CNRS, 45071 Orléans, France
[2] IMT Nord Europe, Institut Mines-Télécom, University Lille, Centre for Energy and Environment, 59000 Lille, France; antoine.roose@imt-nord-europe.fr (A.R.); emmanouil.romanias@imt-nord-europe.fr (M.N.R.)
[3] University Lille, CNRS, UMR 8523-PhLAM-Physique des Lasers Atomes et Molécules, 59000 Lille, France; valerie.vallet@univ-lille.fr
* Correspondence: yuri.bedjanian@cnrs-orleans.fr

Abstract: The kinetics of the F_2 reaction with thiirane (C_2H_4S) was studied for the first time in a flow reactor combined with mass spectrometry at a total helium pressure of 2 Torr and in the temperature range of 220 to 800 K. The rate constant of the title reaction was determined under pseudo-first-order conditions, either monitoring the kinetics of F_2 or C_2H_4S consumption in excess of thiirane or of F_2, respectively: $k_1 = (5.79 \pm 0.17) \times 10^{-12} \exp(-(16 \pm 10)/T)$ cm^3 molecule^{-1} s^{-1} (the uncertainties represent precision of the fit at the 2σ level, with the total 2σ relative uncertainty, including statistical and systematic errors on the rate constant being 15% at all temperatures). HF and CH_2CHSF were identified as primary products of the title reaction. The yield of HF was measured to be 100% (with an accuracy of 10%) across the entire temperature range of the study. Quantum computations revealed reaction enthalpies ranging from −409.9 to −509.1 kJ mol^{-1} for all the isomers/conformers of the products, indicating a strong exothermicity. Boltzmann relative populations were then established for different temperatures.

Keywords: fluorine; C_2H_4S; gas-phase kinetics; rate constant; Boltzmann population; enthalpy

Citation: Bedjanian, Y.; Roose, A.; Vallet, V.; Romanias, M.N. Experimental and Theoretical Study of the Reaction of F_2 with Thiirane. *Molecules* **2024**, *29*, 3636. https://doi.org/10.3390/molecules29153636

Academic Editor: Albin Pintar

Received: 5 July 2024
Revised: 29 July 2024
Accepted: 30 July 2024
Published: 31 July 2024

1. Introduction

The reactivity of F_2 molecules has certain specific features and is of interest for both experimental and theoretical studies. One notable feature is that molecular fluorine exhibits surprisingly high reactivity towards certain closed-shell molecules. For example, it has been demonstrated that reactions of F_2 with organosulfur compounds, CH_3SCH_3 and CH_3SSCH_3, and with limonene are barrierless reactions [1–3]. Unexpectedly high rate constants (for reactions between two closed-shell molecules), 1.6×10^{-11} at 298 K [4] and 1.9×10^{-12} cm^3 molecule^{-1} s^{-1} at T = 278–360 K [3], were reported for reaction of F_2 with dimethyl sulfide (CH_3SCH_3) and limonene, respectively. The current kinetic and mechanistic database on F_2 reactions with stable molecules is very limited [5], especially regarding information on reaction products and the temperature dependence of reaction rate constants. To better understand the nature of the specific reactivity of the F_2 molecule, additional kinetic and mechanistic studies (preferably over a wide temperature range) are necessary.

In the present work, we report the results of combined experimental and theoretical study of the reaction of molecular fluorine with another organosulfur compound, thiirane (C_2H_4S), over a wide temperature range (from 220 to 800 K):

$$F_2 + C_2H_4S \rightarrow \text{products} \quad (1)$$

The reaction rate constant as well as the reaction products are reported for the first time. To our knowledge, no information exists in the literature regarding the spontaneity

and thermodynamical stability of this reaction. Quantum computations have been carried out to determine the thermodynamical parameter of the reaction.

2. Results and Discussion

The reaction of F_2 with C_2H_4S was studied at a total pressure of 2 Torr of He and at temperatures ranging from 220 to 800 K. The configuration of the flow reactors used in the experiments is shown in Figures 1 and S1 (Supplementary Materials). It should be noted that the microwave discharge shown in Figures 1 and S1 was only used in the HF calibration experiments (see experimental section), but was turned off during the kinetic study of the title reaction.

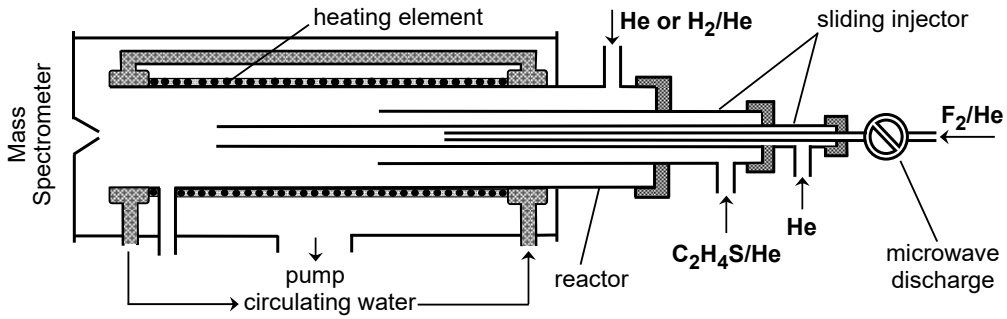

Figure 1. Configuration of the high-temperature flow reactor used in the study of reaction (1).

2.1. Products of Reaction (1)

2.1.1. Measurements of HF Yield

HF and C_2H_3SF were identified as primary products of reaction (1):

$$F_2 + C_2H_4S \rightarrow HF + C_2H_3SF$$

Both species were monitored by mass spectrometry on their parent peaks at m/z = 38 (F_2^+) and 78 ($C_2H_3SF^+$), respectively. Experiments to determine the branching ratio of this reactive channel were carried out with an excess of thiirane over F_2 and consisted of measuring the consumed concentrations of the reactants and those of the two products formed. With the initial C_2H_4S concentrations shown in Table 1 and a reaction time of 0.015 to 0.020 s, the consumed fraction of F_2 (the initial F_2 concentration was varied by a factor of approximately 10) was $\geq$ 90%. The initial concentrations of the two reactants were comparable, allowing the detection of not only the consumption of F_2, but also that of the excess reagent, C_2H_4S.

Table 1. Experimental conditions and results of the measurements of HF yield in reaction (1).

T (K)	$[C_2H_4S]_0$ [a]	$\Delta[F_2]$ [b]	$\Delta[HF]/\Delta[C_2H_4S]$ [c]	$\Delta[HF]/\Delta[F_2]$ [d]
220	3.5–3.8	0.18–1.80	1.04 ± 0.01	1.01±0.01
253	4.5–5.0	0.12–2.08	1.02 ± 0.01	1.01±0.01
298	3.2–5.0	0.19–2.07	1.01 ± 0.02	1.01±0.01
325	4.5–5.0	0.15–2.04	1.06 ± 0.01	1.05 ± 0.01
360	2.0–3.8	0.09–1.51	0.98 ± 0.01	0.95 ± 0.01
500	3.1–3.5	0.10–1.09	1.01 ± 0.01	1.00 ± 0.01
670	2.0–2.5	0.08–0.72	1.02 ± 0.01	1.00 ± 0.01
800	3.32–4.0	0.10–1.89	0.97 ± 0.01	0.96 ± 0.01

[a] Initial concentration of C_2H_4S (units of 10^{13} molecule cm^{-3}); [b] consumed concentration of F_2 (units of 10^{13} cm^3 molecule^{-1} s^{-1}); [c] ratio of [HF] formed to [C_2H_4S] consumed; [d] ratio of [HF] formed to [F_2] consumed. For HF yield statistical 2σ uncertainty is given, total estimated uncertainty is 10%.

Examples of the experimental data observed in these experiments are shown in Figure 2, where the formed concentrations of the reaction products are plotted against

the [F_2] and [C_2H_4S] consumed. Note that the concentrations of C_2H_3SF in Figure 2 are presented in relative units; absolute concentrations were measured only for HF. The yields of HF determined from the slopes of the black lines in Figure 2 ([HF]/Δ[F_2] and [HF]/Δ[C_2H_4S]) at different temperatures are listed in Table 1. The results show that one molecule of HF is formed per one molecule of F_2 and C_2H_4S consumed. This observation, along with the linearity of the corresponding plots for C_2H_3SF, seems to indicate a negligible impact of possible secondary and side reactions under the experimental conditions of the measurements and that the HF + C_2H_3SF forming channel is the main, if not only, reaction pathway in the entire temperature range of the study (220–800 K). Combining the statistical uncertainty of measurements with the accuracy of measuring the absolute concentrations of F_2, C_2H_4S and HF of around 5%, a branching ratio equal to unity with an error of 10% can be recommended for the HF forming channel of reaction (1).

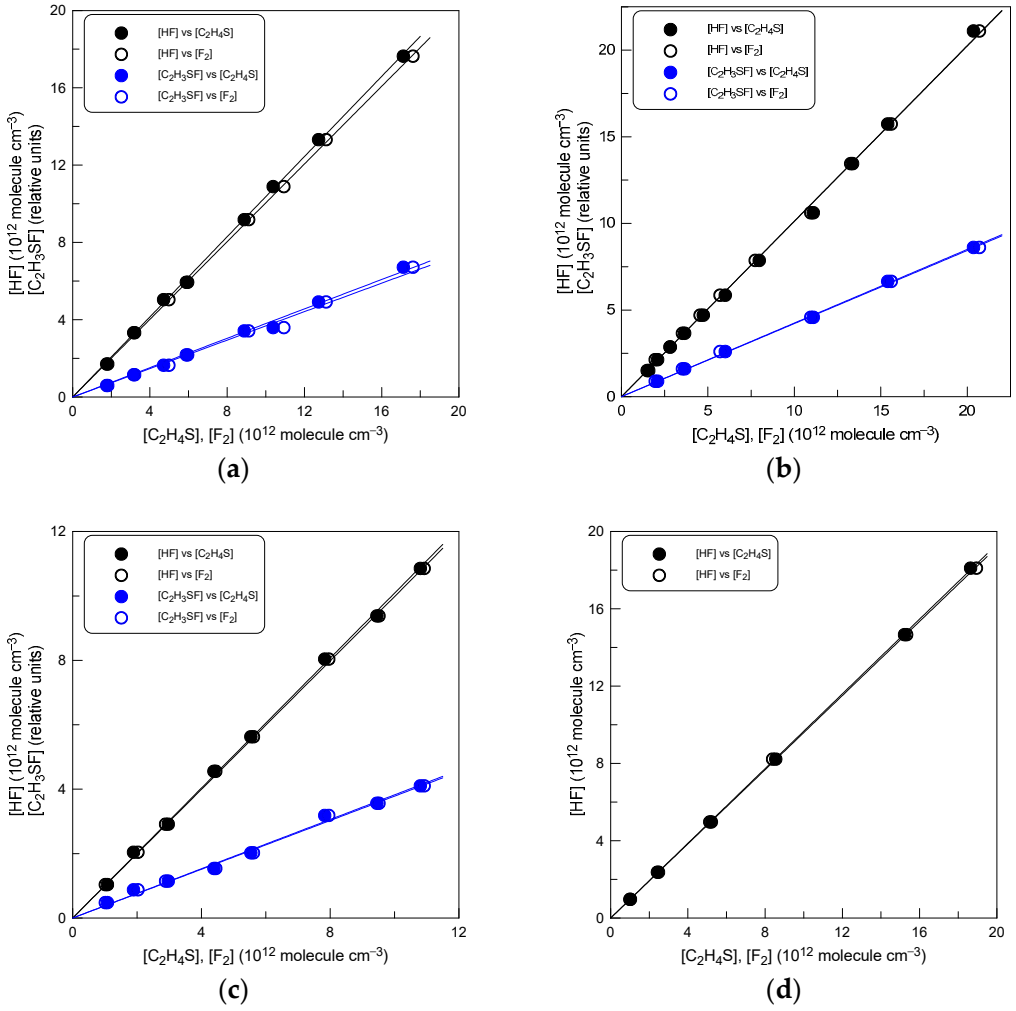

Figure 2. Concentration of the products, HF and C_2H_3SF, formed in reaction (1) as a function of the consumed concentration of the reactants, C_2H_4S and F_2: (**a**) T = 220 K; (**b**) T = 298 K; (**c**) T = 500 K; and (**d**) T = 800 K.

As previously noted, all measurements were carried out with an excess of C_2H_4S. The fact is that in an excess of F_2, we observed signs of a secondary reaction of F_2 with C_2H_3SF. The kinetics of C_2H_3SF exhibited a characteristic behavior: [C_2H_3SF] initially increased to a maximum and then decreased due to the secondary reaction with F_2. Concurrently, we observed the formation of SF_2 (at m/z = 70). Studying this secondary reaction was beyond the scope of this work, so we limited the branching ratio measurements to experiments with excess of C_2H_4S, where the secondary chemistry could be neglected. However, it

should be noted that at T = 800 K (the highest temperature of the study), we observed evidence of C_2H_3SF removal, albeit slowly, even in the absence of F_2 in the reactor. We are inclined to think that this is due to thermal decomposition of C_2H_3SF, although other processes of C_2H_3SF removal cannot be ruled out. For this reason, in Figure 2d we do not present the measurements of [C_2H_3SF].

The structure of the C_2H_3SF formed in reaction (1) was not determined, but some considerations can nevertheless be discussed. Most probably, reaction (1) proceeds through the addition of F_2 to the sulfur atom followed by the elimination of HF, as proposed by Nelson et al. [6]:

$$F_2 + C_2H_4S \rightarrow [C_2H_4S(F\text{-}F)]^* \rightarrow HF + C_2H_3SF$$

In this case, the most likely product is CH_2=CH-SF (ethenyl thiohypofluorite). Mass spectrometry analysis of C_2H_3SF (formed in reaction (1)) revealed a prominent fragment peak at m/z = 51 (SF^+), which, although indirectly, supports this hypothesis. The presence of this peak in the mass spectrum of other conformers, for example, 2-fluorotiirane or S=CH-CH_2F, seems to be unlikely. In addition, signals at m/z = 63 and 64, which can be attributed to C-SF^+ and CH-SF^+, respectively, are observed and are consistent with the mass spectrometric fragments of CH_2=CHSF.

For the analogous reaction of F_2 with DMS, Turnipseed and Birks [4] observed a reaction product, thought to be H_2C=S(F)CH_3, when DMS was in excess over F_2. This product was found to be destroyed in an excess of F_2 in the reactor, similar to how CH_2=CH-SF behaves in the present work. The authors proposed that the reaction proceeds through a charge-transfer complex with subsequent elimination of H and F atoms or of molecular HF. The HF production channel was thought to constitute a small part of the reaction pathway, although there was no experimental evidence for that. In contrast, for the F_2 reaction with C_2H_4S investigated in the present work, a significant contribution of the F atom forming channel can apparently be excluded, given that in an excess of thiirane it was observed that [HF] = Δ[F_2] = Δ[C_2H_4S].

2.1.2. Theoretical Findings

The enthalpies (including Zero-Point Energy, ZPE) and Gibbs free energies of the thiirane reaction with F_2 were computed for all possible isomers and conformers of the products C_2H_3FS (Table 2). These isomers and conformers (for the case of 2-fluoroethenethiol) are shown in Figure 3. The computed reaction enthalpies range from -509.1 kJ mol^{-1} (for the case of thioacetylfluoride) to -409.9 kJ mol^{-1} (in the case of Ethenylhypofluorite). The Gibbs free energies are in the same order of magnitude, indicating a spontaneous reaction.

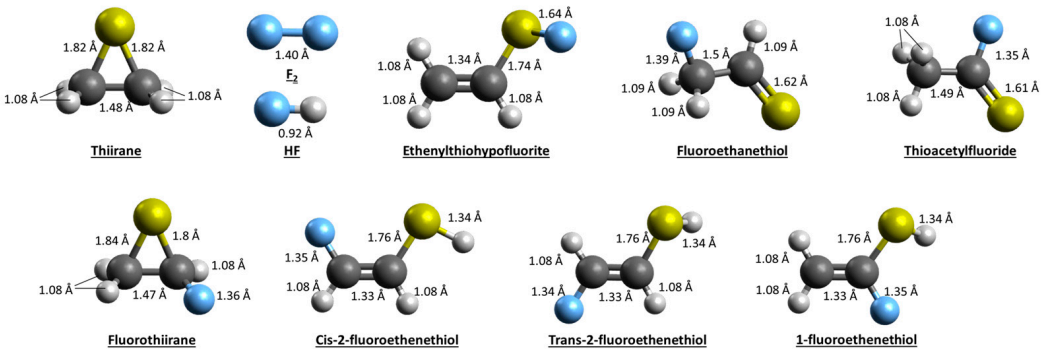

Figure 3. Geometries of the reactants and C_2H_3SF isomers/conformers optimized at the MP2/aug-cc-pVTZ level of theory. Sulfur atoms are yellow, fluorine in blue, carbon atoms in dark gray and hydrogen in light gray.

Table 2. Summary of the enthalpies (in kJ/mol, including the ZPE correction), Gibbs free energies and Boltzmann population for the isomers and conformers at temperature of 298, 500 and 1000 K, computed at the CCSD(T)-CBS/(aug-cc-pVTZ:aug-cc-pVQZ)//MP2/aug-cc-pVTZ level.

Molecule	ΔG (kJ/mol)	ΔH (kJ/mol)	Boltzmann Population T = 298 K	Boltzmann Population T = 500 K	Boltzmann Population T = 1000 K
1-fluoroethenethiol	−470.7	−473.1	2.0×10^{-7}	1.0×10^{-4}	9.8×10^{-3}
Cis-2-fluoroethenethiol	−467.1	−467.8	2.4×10^{-8}	2.9×10^{-5}	5.2×10^{-3}
Ethenylthyohypofluorite	−409.9	−411.3	3.0×10^{-18}	3.6×10^{-11}	5.9×10^{-6}
Fluoroethanethiol	−456.3	−456.6	2.6×10^{-10}	1.9×10^{-6}	1.4×10^{-3}
Fluorothiirane	−462.0	−466.2	1.3×10^{-8}	2.0×10^{-5}	4.3×10^{-3}
Thioacetylfluoride	−509.1	−511.3	1	1	9.8×10^{-1}
Trans-2-fluoroethenethiol	−463.4	−465.5	9.3×10^{-9}	1.6×10^{-5}	4.0×10^{-3}

From the energies of the different products, we can compute the relative Boltzmann population as function of the temperature using the following equation:

$$Boltzmann\ population = e^{\frac{\Delta H}{RT}} / \sum e^{\frac{\Delta H}{RT}}$$

with ΔH being the relative enthalpy, R the gas constant and T the temperature. The Boltzmann population analysis indicates that thioacetylfluoride is the predominant species formed, with 1-fluoroethenethiol being the second most abundant species. These species could be source of CHSF and CSF fragments but not of the SF fragment, which was observed experimentally. It should be noted that calculations provide insights into the thermochemistry, pointing to a highly exergonic reaction, but not into the kinetics, since the energy barrier of the transition states was not calculated. Given the exergonic nature of the reaction, products that have high energy barriers, or include rearrangements, and could proceed through multiple transition states may not be kinetically favored.

2.2. Measurements of the Rate Constant of Reaction (1)

In most experiments, the reaction rate constant was determined from the kinetics of C_2H_4S consumption ($[C_2H_4S]_0 = (1.5 - 5.0) \times 10^{11}$ molecule cm^{-3}), monitored in an excess of F_2 in the reactor (for concentrations of F_2 see Table 3).

Table 3. Summary of the measurements of the rate constant of reaction (1).

T (K) [a]	Excess Reactant	[Excess Reactant] [b]	$k_1(\pm 2\sigma)$ [c]	Reactor Surface [d]
220	F_2	0.52–5.35	6.30 ± 0.08	HW
235	F_2	0.39–4.70	6.28 ± 0.09	HW
253	F_2	0.39–5.53	6.15 ± 0.06	HW
265	C_2H_4S	0.24–4.82	6.34 ± 0.05	HW
275	F_2	0.30–4.60	6.06 ± 0.06	HW
298	F_2	0.36–5.45	5.92 ± 0.07	HW
315	C_2H_4S	0.23–2.31	6.22 ± 0.09	Q
325	F_2	0.18–5.24	5.91 ± 0.09	HW
340	F_2	0.20–4.00	6.00 ± 0.06	Q
360	F_2	0.36–4.02	6.03 ± 0.07	Q
390	F_2	0.35–4.68	6.13 ± 0.10	Q
420	C_2H_4S	0.22–1.94	5.87 ± 0.05	Q
460	F_2	0.36–3.69	6.06 ± 0.12	Q
500	F_2	0.29–3.19	5.86 ± 0.06	Q
560	F_2	0.22–3.30	5.83 ± 0.11	Q
625	C_2H_4S	0.18–1.73	6.07 ± 0.06	Q
710	F_2	0.21–2.88	6.03 ± 0.09	Q
800	F_2	0.27–2.51	5.99 ± 0.06	Q

[a] 8–12 decay traces at each temperature; [b] units of 10^{13} molecule cm^{-3}; [c] units of 10^{-12} cm^3 molecule^{-1} s^{-1}, statistical 2σ uncertainty is given, total estimated uncertainty of k_1 is 15%; [d] HW: halocarbon wax; Q: quartz.

Examples of observed C_2H_4S decays are shown in Figure 4. The temporal profiles of C_2H_4S were fitted to an exponential function $[C_2H_4S] = [C_2H_4S]_0 \times \exp(-k_1' \times t)$, where $[C_2H_4S]_0$ and $[C_2H_4S]$ are the initial and time-dependent concentrations of thiirane, respectively, and $k_1' = k_1 \times [F_2]$ is the pseudo-first-order rate constant. The diffusion corrections made in [7] to the k_1' values measured in this way were less than 10%.

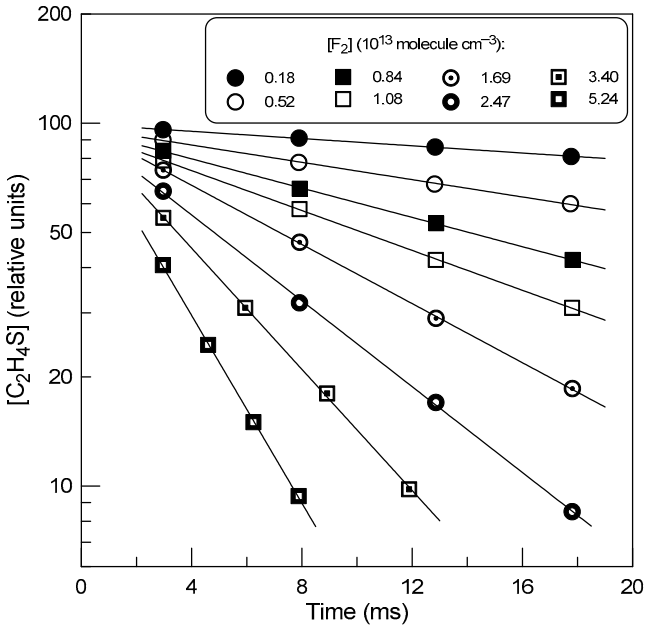

Figure 4. Example of the kinetics of C_2H_4S consumption in reaction (1) at different concentrations of F_2 observed at T = 325 K.

Examples of second-order plots measured at different temperatures are shown in Figure 5. A linear least-square fit through the origin of the k_1' data as a function of $[F_2]$ provides the rate constant of reaction (1) at the corresponding temperature. All the results obtained for k_1 are given in Table 3.

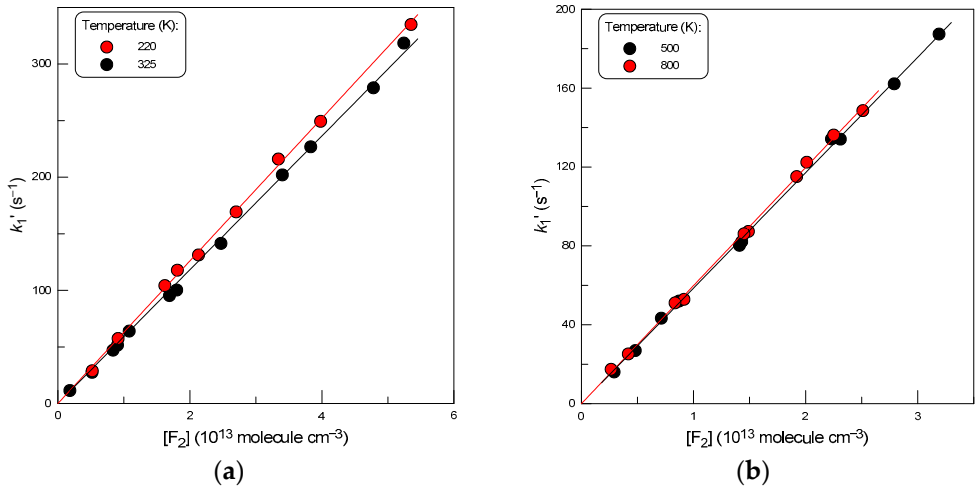

Figure 5. Pseudo-first-order rate constant, $k_{1'} = k_1 \times [F_2]$, as a function of F_2 concentration at different temperatures: (**a**) T = 220 and 325 K; (**b**) T = 500 and 800 K.

In some experiments, the rate constant of reaction (1) was determined from the kinetics of F_2 consumption monitored in an excess of thiirane in the reactor. The initial concentration of F_2 in these experiments was $\leq 10^{12}$ molecule cm^{-3}. The observed C_2H_4S consumption (within a few %) was taken into account by using the average C_2H_4S concentration over

the reaction zone. Examples of second-order plots and final values of k_1 obtained in this series of experiments are shown in Figure 6 and Table 3, respectively.

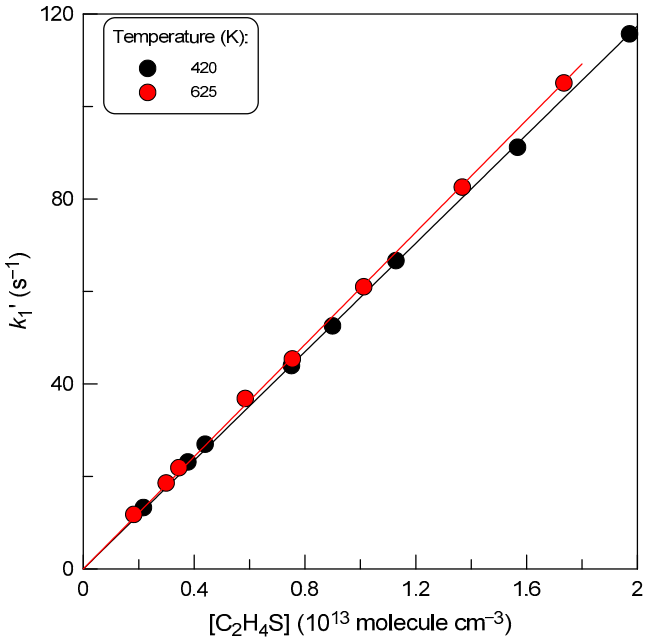

Figure 6. Pseudo-first-order rate constant, $k_{1'} = k_1 \times [C_2H_4S]$, as a function of C_2H_4S concentration observed at T = 420 and 625 K.

The results of all k_1 measurements are summarized in Figure 7.

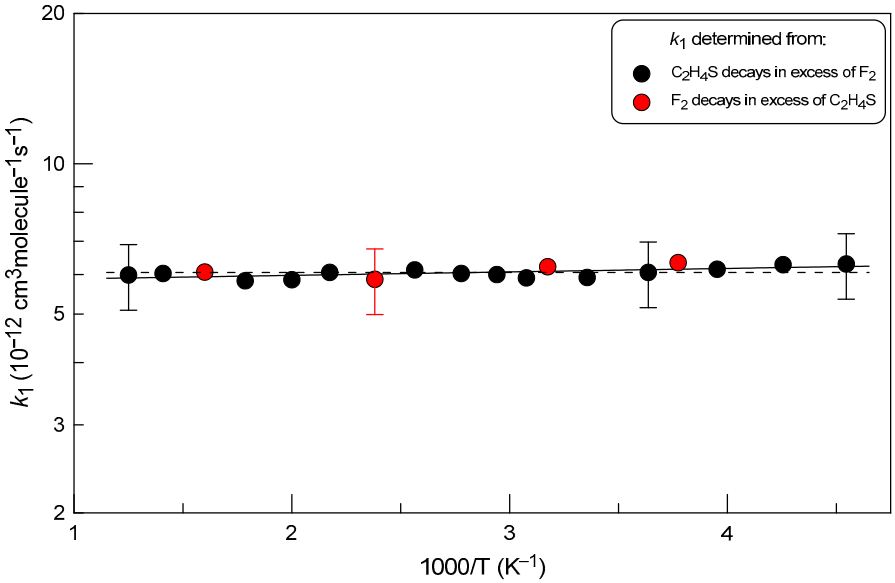

Figure 7. Temperature dependence of the rate constant of reaction (1). Partially shown error bars correspond to estimated total uncertainty of 15% on the measurements of k_1.

It can be noted that there is an excellent agreement between the data obtained under different experimental conditions, from F_2 and C_2H_4S kinetics in excess of C_2H_4S and F_2, respectively. Fitting the dependence of k_1 on temperature to the exponential function (solid line in Figure 6) gives the following Arrhenius expression:

$$k_1 = (5.79 \pm 0.17) \times 10^{-2} \exp(-(16 \pm 10)/T) \text{ cm}^3 \text{ molecule}^{-1} \text{ s}^{-1}$$

at T = 220–800 K with 2σ uncertainties representing the precision of the fit. We estimate this expression to be accurate within an overall 2σ uncertainty of 15% over the investigated temperature range. Considering the virtual independence of the rate constant of temperature, the temperature independent value of

$$k_1 = (6.05 \pm 0.90) \times 10^{-12} \text{ cm}^3 \text{ molecule}^{-1} \text{ s}^{-1}$$

can be recommended for the rate constant of reaction (1) (dashed line in Figure 6) in the temperature range (220−800) K. The observed temperature independence of k_1 appears to be consistent with a reaction mechanism consisting of barrier-free formation of an intermediate followed by its decomposition into reactants or reaction products.

Turnipseed and Birks [4] in their study of the F_2+DMS reaction speculated that the reaction can be initiated by the transfer of an electron from the sulfur compound to F_2, forming a charge-transfer complex. Considering that the electron transfer process must be either exothermic or thermoneutral for the reaction to proceed at a measurable rate they calculated a critical distance, $r_c = 14.4/(\text{IP(reactant)} - \text{EA}(F_2))$, which corresponds to the maximum distance at which the charge-transfer complex can be stable and the electron can be transferred (EA(F_2): electron affinity of molecular fluorine; IP(reactant): ionization potential of the second reactant). By analyzing the r_c for F_2 interactions with a number of compounds, the authors estimated that a critical distance greater than 2.3 Å is required for the reaction to occur [4]. The present data for the reaction of F_2 with thiirane are consistent with this reasoning, given that r_c = 2.4 Å (calculated with IP(C_2H_4S) = 9.05 eV [8] and EA(F_2) = 3.08 eV [9]) and a relatively high value was measured for the reaction rate constant.

3. Materials and Methods

3.1. Experimental

The experimental setup consisted of a discharge flow reactor combined with a modulated molecular beam mass spectrometer with electron impact ionization operated at 30 eV energy (Figure 1) [10,11]. The reaction time was determined by the position of the movable injector relative to the sampling cone of the mass spectrometer; changing its position makes it possible to vary the reaction time. Linear flow velocities in the reactor ranged from 1730 to 2400 cm s^{-1}. The chemical composition of the reactive system was monitored by sampling gas-phase molecules from the flow reactor and detecting them with a mass spectrometer. All species involved were detected at their parent peaks.

Two flow reactors were used in this study to cover a wide temperature range for kinetic measurements. The first reactor, operated at high temperatures (315–800 K), consisted of an electrically heated quartz tube (45 cm length and 2.5 cm i.d.) with water-cooled attachments (Figure 1) [12]. The temperature in the reactor was measured with a K-type thermocouple positioned in the middle of the reactor in contact with its outer surface [12]. The second flow reactor (Figure S1) used at lower temperatures (220–325 K) consisted of a Pyrex tube (45 cm length and 2.4 cm i.d.); temperature regulation was achieved by circulating thermostated ethanol. The walls of the Pyrex reactor, as well as the mobile injector of fluorine atoms, were coated with halocarbon wax to prevent the reaction of the F atom with the glass surface.

The absolute concentrations of F_2, H_2 and C_2H_4S were calculated from their flow rates, obtained from pressure drop measurements of their mixtures in He stored in calibrated volume flasks. Absolute calibration of the mass spectrometer to HF was carried out by titrating a known concentration of H_2 with an excess of F atoms ([HF] = [H_2]) in a fast reaction:

$$F + H_2 \rightarrow HF + H \quad (2)$$

$k_2 = 1.24 \times 10^{-10} \exp(-507/T)$ cm^3 molecule^{-1} s^{-1} (T = 220–960 K) [13]. Fluorine atoms in these experiments were generated in a microwave discharge of trace amounts of F_2 in He. It was verified by mass spectrometry that more than 95% of F_2 was dissociated in

the microwave discharge. To reduce F atom reactions with the glass surface inside the microwave cavity, a ceramic (Al_2O_3) tube was inserted in this part of the injector.

The purities of the gases used were as follows: He (>99.9995%, Alphagaz, Air Liquide, Paris, France), passed through liquid nitrogen trap; H_2 (> 99.998%, Alphagaz); and F_2, 5% in helium (Alphagaz); C_2H_4S (Merck, Merck SA, Lyon, France), 98%.

3.2. Computational Methodology

In order to select the correct methodology to perform the computation, a thorough benchmark was carried out. Based on Vila et al. [14], we used density functional theory (DFT) with a B3LYP function in comparison with the Schrödinger-based MP2 method and CCSD method, which is used as reference, having the highest level of accuracy among the benchmarked methods. In practice, DFT, MP2 and CCSD calculations were performed with the Gaussian 16 software [15], while the more time-consuming CCSD(T)-CBS calculations were carried out using the Molpro 2023.2.0 software [16–18].

B3LYP and MP2 methods were compared using the same basis set (6-311++G(3d2f,3p2d)) as the CCSD methodology. The criteria to determine the accuracy of B3LYP and MP2 compared to CCSD were based on the geometries of the molecules and their energies once corrected with single-point computation at the same level of methodology as when using CCSD(T) with a CBS correction (aug-cc-pVTZ:aug-cc-pVQZ). In Figure S2, the energy differences are introduced and it is shown that only the MP2 method remains with differences under chemical accuracy (4.18 kJ/mol). Figures S3–S10 illustrate the geometry differences for each product, showing negligible discrepancies in bond lengths (maximum of 0.02 Å), indicating the minimal impact of the method on this parameter. Concerning angles, small differences are observed with a maximum of 1.28 degrees. However, we can start to observe some indication that MP2 is slightly better than B3LYP to reproduce the angles. Finally, concerning dihedral angles, strong differences can be observed in the case of the B3LYP methodology compared to MP2. Indeed, in the case of cis-2-fluoroethenethiol, ethenylthiohypofluorite and fluoroethanethial some dihedral angles increase a lot (up to 127.55 degrees) in the case of B3LYP. Such differences indicate a clear change in the configuration of the molecule. In MP2, the differences are up to 7.02 degrees, which is more reasonable. In conclusion, the MP2 methodology seems more reliable in comparison to the CCSD method. The computational cost increases slightly compared to DFT but is still reasonable compared to the CCSD methodology, which is prohibitively expensive.

Using both B3LYP and MP2, which are reasonable in terms of computational cost, the 6-311++G(3d2f,3p2d) and aug-cc-pVDZ were compared to the aug-cc-pVTZ basis set, which is the largest among the three. Geometries and energies are compared, as they are in the benchmark of the method. In Figure S11, energy differences clearly indicate that basis set size has an effect, as the energy is above chemical accuracy in the case of 6-311++G(3d2f,3p2d) and for ethenylthiohypofluorite with the aug-cc-pVDZ. Figures S12–S19 introduce geometry differences. It is evident that the 6-311++G(3d2f,3p2d) basis set struggles to accurately represent bonds involving sulfur and fluorine atoms. It is even more remarkable in the case of ethenylthiohypofluorite, where the error is around 0.16 Å (B3LYP) and 0.18 Å (MP2). These differences can significantly impact the calculated energies. Dihedral angles are notably impacted by the size of the basis set for both methods. Therefore, the larger aug-cc-pVTZ basis set is recommended.

Supplementary Materials: The following supporting information can be downloaded at: https://www.mdpi.com/article/10.3390/molecules29153636/s1, Figure S1: configuration of the low-temperature flow reactor; Figure S2: single-point energy differences between B3LYP, MP2 and CCSD methods; Figures S3–S10: bond length differences calculated with different methods; Figure S11: single-point energy differences for different basis set sizes; Figures S12–S19: geometry differences between different basis sets; Figure S20: Boltzmann relative distribution of the reaction products as a function of temperature; optimized geometry; inputs.

Author Contributions: Conceptualization, experimental investigation, data analysis and interpretation, writing, Y.B.; computation, methodology, validation, formal analysis, writing, A.R.; validation, writing, supervision, V.V.; review, editing, supervision, M.N.R. All authors have read and agreed to the published version of the manuscript.

Funding: This research was partly funded by ANR through the PIA (Programme d'Investissement d'Avenir, grant number ANR-10-LABX-100-01), Labex CaPPA, funded by ANR through the PIA under contract ANR-11-LABX-0005-01, and CPER ECRIN project, both funded by the Hauts-de-France Regional Council and the European Regional Development Fund (ERDF).

Institutional Review Board Statement: Not applicable.

Informed Consent Statement: Not applicable.

Data Availability Statement: The data supporting reported results are available in this article.

Conflicts of Interest: The authors declare no conflicts of interest.

References

1. Lu, Y.-J.; Lee, L.; Pan, J.-W.; Xie, T.; Witek, H.A.; Lin, J.J. Barrierless reactions between two closed-shell molecules. I. Dynamics of F_2+CH_3SCH_3 reaction. *J. Chem. Phys.* **2008**, *128*, 104317. [CrossRef] [PubMed]
2. Shao, H.-C.; Xie, T.; Lu, Y.-J.; Chang, C.-H.; Pan, J.-W.; Lin, J.J. Barrierless reactions between two closed-shell molecules. II. Dynamics of F_2+CH_3SSCH_3 reaction. *J. Chem. Phys.* **2009**, *130*, 014301. [CrossRef] [PubMed]
3. Bedjanian, Y.; Romanias, M.N.; Morin, J. Reaction of Limonene with F_2: Rate Coefficient and Products. *J. Phys. Chem. A* **2014**, *118*, 10233–10239. [CrossRef] [PubMed]
4. Turnipseed, A.A.; Birks, J.W. Kinetics of the reaction of molecular fluorine with dimethyl sulfide. *J. Phys. Chem.* **1991**, *95*, 6569–6574. [CrossRef]
5. Manion, J.A.; Huie, R.E.; Levin, R.D.; Burgess, D.R.; Orkin, V.L.; Tsang, W.; McGivern, W.S.; Hudgens, J.W.; Knyazev, V.D.; Atkinson, D.B.; et al. NIST Chemical Kinetics Database, NIST Standard Reference Database 17, Version 7.0 (Web Version), Release 1.6.8, Data version 2015.12, National Institute of Standards and Technology, Gaithersburg, Maryland, 20899-8320. Available online: http://kinetics.nist.gov/ (accessed on 3 July 2024).
6. Nelson, J.K.; Getty, R.H.; Birks, J.W. Fluorine induced chemiluminescence detector for reduced sulfur compounds. *Anal. Chem.* **1983**, *55*, 1767–1770. [CrossRef]
7. Kaufman, F. Kinetics of elementary radical reactions in the gas phase. *J. Phys. Chem.* **1984**, *88*, 4909–4917. [CrossRef]
8. Butler, J.J.; Baer, T. A photoionization study of organosulfur ring compounds—Thiirane, thietane and tetrahydrothiophene. *Org. Mass Spectrom.* **1983**, *18*, 248–253. [CrossRef]
9. Bartmess, J.E.; McIver, R.T. Chapter 11—The gas-phase acidity scale. In *Gas Phase Ion Chemistry*; Bowers, M.T., Ed.; Academic Press: Cambridge, MA, USA, 1979; pp. 87–121.
10. Bedjanian, Y. Rate Coefficients of the Reactions of Fluorine Atoms with H_2S and SH over the Temperature Range 220–960 K. *Molecules* **2022**, *27*, 8365. [CrossRef] [PubMed]
11. Bedjanian, Y. Temperature-Dependent Kinetic Study of the Reactions of Hydrogen Atoms with H_2S and C_2H_4S. *Molecules* **2023**, *28*, 7883. [CrossRef] [PubMed]
12. Morin, J.; Romanias, M.N.; Bedjanian, Y. Experimental study of the reactions of OH radicals with propane, *n*-pentane, and *n*-heptane over a wide temperature range. *Int. J. Chem. Kinet.* **2015**, *47*, 629–637. [CrossRef]
13. Bedjanian, Y. Rate constants for the reactions of F atoms with H_2 and D_2 over the temperature range 220–960 K. *Int. J. Chem. Kinet.* **2021**, *53*, 527–535. [CrossRef]
14. Vila, A.; Puente, E.d.l.; Mosquera, R.A. QTAIM study of the electronic structure and strain energy of fluorine substituted oxiranes and thiiranes. *Chem. Phys. Lett.* **2005**, *405*, 440–447. [CrossRef]
15. Frisch, M.J.; Trucks, G.W.; Schlegel, H.B.; Scuseria, G.E.; Robb, M.A.; Cheeseman, J.R.; Scalmani, G.; Barone, V.; Petersson, G.A.; Nakatsuji, H.; et al. *Gaussian 16*, Rev. C.01; Gaussian, Inc.: Wallingford, CT, USA, 2016.
16. Werner, H.-J.; Knowles, P.J.; Manby, F.R.; Black, J.A.; Doll, K.; Heßelmann, A.; Kats, D.; Köhn, A.; Korona, T.; Kreplin, D.A.; et al. The Molpro quantum chemistry package. *J. Chem. Phys.* **2020**, *152*. [CrossRef] [PubMed]
17. Werner, H.-J.; Knowles, P.J.; Knizia, G.; Manby, F.R.; Schütz, M. Molpro: A general-purpose quantum chemistry program package. *WIREs Comput. Mol. Sci.* **2012**, *2*, 242–253. [CrossRef]
18. Werner, H.-J.; Knowles, P.J.; Celani, P.; Györffy, W.; Hesselmann, A.; Kats, D.; Knizia, G.; Köhn, A.; Korona, T.; Kreplin, D.; et al. MOLPRO, Version, a Package of ab Initio Programs. Available online: https://www.molpro.net (accessed on 3 July 2024).